The Osmotic Rupture Hypothesis of Intracellular Freezing Injury

Ken Muldrew and Locksley E. McGann
Department of Laboratory Medicine and Pathology, University of Alberta, Edmonton, Alberta, Canada T6G 2R7

ABSTRACT A hypothesis of the nature of intracellular ice formation is proposed in which the osmotically driven water efflux that occurs in cells during freezing (caused by the increased osmotic pressure of the extracellular solution in the presence of ice) is viewed as the agent responsible for producing a rupture of the plasma membrane, thus allowing extracellular ice to propagate into the cytoplasm. This hypothesis is developed into a mathematical framework and the forces that are present during freezing are compared to the forces which are required to rupture membranes in circumstances unrelated to low temperatures. The theory is then applied to systems which have been previously studied to test implications of the theory on the nature of intracellular ice formation. The pressure that develops during freezing due to water flux is found to be sufficient to cause a rupture of the plasma membrane and the theory gives an accurate description of the phenomenology of intracellular ice formation.

INTRODUCTION

There has recently been renewed interest in the phenomenon of intracellular ice formation (the freezing of cytoplasm which is usually associated with lethal injury) in cells exposed to low temperatures. Phenomenological models of intracellular ice formation have been proposed which use statistical information to predict the likelihood of intracellular ice formation during defined freezing protocols (Mazur, 1977; Pitt and Steponkus, 1989). Mechanistic models have also been proposed, based on two general views: that intracellular ice formation is the *cause* of injury to the cell or that it is a *result* of damage to the plasma membrane. The former approach, most recently applied in a theory proposed by Toner et al. (1990), suggests that intracellular ice formation occurs as a result of nucleation within the cell, catalyzed either by the plasma membrane or intracellular particles. An alternate hypothesis, proposed by Muldrew and McGann (1990), contends that osmotic stresses which develop during cooling lead to a rupture in the plasma membrane which then allows extracellular ice to propagate into the cytoplasm. Mazur (1960, 1966) has long held the view that intracellular ice formation is seeded by extracellular ice, although it is not the result of a rupture in the plasma membrane. His hypothesis maintains that when a critical temperature is encountered during cooling, at which the smallest radius of stable ice crystal growth matches the radius of aqueous pores in the plasma membrane, then intracellular ice formation will occur if there is supercooled water in the cytoplasm.

It is important that the mechanisms of freezing injury be understood if techniques are to be developed which avoid this injury. Although purely empirical approaches have been successful in developing cryopreservation protocols for cell suspensions and a few simple tissue systems, these have not resulted in techniques for cryopreserving complex mammalian tissues. Success in this area would have obvious benefits in medicine as it would allow banking of tissues and organs for transplantation. Current approaches to tissue and organ preservation use high concentrations of cryoprotective compounds and rapid rates of cooling, conditions under which high osmotic stresses and intracellular ice formation are likely to occur. Due to the complex set of interacting variables in these approaches, many researchers have now turned to mathematical modeling of organized tissues at low temperatures to predict responses and optimize protocols. Current models concentrate on describing the response of the tissue to osmotic events that occur during freezing. Although detailed models have been constructed for several tissue systems (Bischof and Rubinsky, 1991; Diller et al., 1991; Rubinsky and Pegg, 1988), there has not been a theoretical foundation of cell damage to allow these models to be used to predict the conditions that could result in lethal injury to the tissue. Hypotheses of freezing injury that relate the mechanism of injury to events which can be modeled during freezing and thawing can be used as tools toward predicting successful protocols in which injury to the tissue is minimized. Mechanistic models have the further advantage of providing physical insight into the systems being studied which may lead to novel solutions which could not have been foreseen from strictly phenomenological models or a purely empirical approach.

The cellular environment during freezing

Mammalian cells necessarily exist in an ionic environment which becomes concentrated during freezing due to the removal of water from the solution in the form of ice. The increased osmotic pressure in the extracellular space creates an osmotic gradient across the cell's plasma membrane which provides a driving force for water efflux from the cell, as described in the conceptual approach introduced by Mazur (Mazur, 1963; Mazur et al., 1984). The rate of water efflux is limited by the membrane's permeability to water, thus it

Received for publication 11 August 1993 and in final form 22 November 1993.

Address reprint requests to Locksley E. McGann at Department of Laboratory Medicine and Pathology, University of Alberta, Edmonton, Alberta, Canada T6G 2R7.

0006-3495/94/02/532/10 $2.00

is possible to cool cells under conditions where the rate of water efflux is insufficient to maintain osmotic equilibrium between the cytoplasm and the unfrozen component of the extracellular solution. Under these conditions, the cytoplasm becomes supercooled and can freeze: an event known as intracellular ice formation (IIF) which can be observed microscopically as a sudden darkening (flashing) of the cytoplasm due to the formation of small ice crystals or microscopic gas bubbles which scatter light (Steponkus and Dowgert, 1981). Intracellular freezing is almost always associated with a lethal injury to the cell, however, there is continuing debate as to whether this injury is a cause or a result of IIF (Muldrew and McGann, 1990; Toner et al., 1990).

Recent experimental work has led us to agree with the suggestion that IIF is the result of a rupture in the plasma membrane which allows extracellular ice to propagate into the supercooled cytoplasm (Dowgert and Steponkus, 1983; Steponkus and Dowgert, 1981). We have proposed that this rupture is due to osmotic pressure gradients which develop across the plasma membrane during rapid cooling (Muldrew and McGann, 1990). The tentative mechanism of this rupture was proposed to be due to the frictional drag of water, which exceeds the tensile strength of the plasma membrane and leads to structural failure (Muldrew and McGann, 1990). Membrane rupture then allows extracellular ice to rapidly propagate into the supercooled cytoplasm, resulting in the flashing commonly observed.

Frictional drag of water during osmotic shrinkage

Water movement across the plasma membrane occurs through a combination of diffusion through the lipid bilayer and movement through transmembrane pores which span the bilayer. There are cell types which are known to use pores as the primary route for water movement. For example, red blood cells and the cells in the renal collecting ducts of the kidney have a water pore protein that has recently been identified (Denker et al., 1988; Preston et al., 1992). Extensive screening of the mRNA for this chip28 protein in cells from other human tissues has shown that this pore is likely to be unique to these two cell types (Zhang et al., 1990); hence the movement of water through pores which exist specifically for this purpose is not typical of mammalian cells (Finkelstein, 1987). Ion channels may allow water movement, possibly as hydrated ions, but there is no evidence that these form the major pathway for osmotic water movement. It has also been shown that pure lipid bilayers can be constructed with water permeabilities which encompass the entire range found in mammalian cells where variation in the composition of the constituent lipids alters the permeability (Finkelstein, 1987), validating the assumption that diffusion through the bilayer is the primary mode of osmotic water movement across the plasma membrane in most mammalian cells. It is important to note that the theory presented here can be extended to cells in which water flux occurs predominantly through pores. The derivation of the frictional drag would require assumptions about the number, distribution, and size of the aqueous pores, since this information is not yet well established.

Water movement through lipid bilayers occurs through a solubility-diffusion mechanism (Bacic et al., 1990; Finkelstein, 1987). When a concentration gradient exists, the water enters the bilayer according to its partition coefficient and then moves down this gradient to the opposite side (Finkelstein, 1987). Each water molecule that moves through the bilayer will impart a frictional force on the bilayer due to collisions with the lipid molecules. The partition coefficient for water in liquid hydrocarbon is large enough that water molecules in the membrane act independently of one another (there is insignificant water-water interaction within the bilayer (Finkelstein, 1987)). The frictional force imparted by a single water molecule will therefore be proportional to the velocity of that molecule as it moves through the hydrophobic region of the bilayer. We can define the drift velocity of a water molecule moving through the bilayer as

$$v = \frac{\Delta x}{\Delta t} \tag{1}$$

where v is drift velocity of a water molecule in the membrane (m/s), Δx is width of the hydrophobic region of the membrane (m), and Δt = average transit time for a water molecule in the membrane (s). The water flux is defined as the number of water molecules moving through the membrane per unit time.

$$J_w = \frac{n}{\Delta t} \tag{2}$$

where J_w is water flux (molecules/s) and n represents the number of water molecules moving through the membrane in time Δt (molecules). Thus, the drift velocity of a water molecule can be expressed as

$$v = \frac{J_w \cdot \Delta x}{n}. \tag{3}$$

The frictional force per molecule is proportional to the drift velocity of a water molecule

$$\frac{F_f}{n} = f \cdot v \tag{4}$$

where F_f is total force on the membrane due to friction of water (N), f is coefficient of friction (defined by Eq. 4) (N · s/m). The frictional force of water in the membrane can therefore be expressed as

$$F_f = f \cdot J_w \cdot \Delta x. \tag{5}$$

Einstein explained diffusion in terms of friction between molecules (Einstein, 1956), and developed an equation relating the microscopic frictional coefficient to the macroscopic diffusion coefficient for the situation in which molecules collide with a sphere which is large compared to the molecules. Levitt has described a more general derivation of

this equation, showing that it is valid for molecules diffusing through a molecular membrane (Levitt, 1974)

$$f = \frac{kT}{D_w} \tag{6}$$

where k is Boltzmann's constant (N · m/K), T is absolute temperature (K), and D_w is the diffusion coefficient for water in liquid hydrocarbon (m^2/s). For water moving through a cell membrane, the diffusion coefficient of water in liquid hydrocarbon has been shown to describe diffusion of water within the hydrophobic region of the bilayer (Finkelstein, 1987).

Therefore the frictional force on the membrane is

$$F_f = \frac{kT}{D_w} \cdot J_w \cdot \Delta x. \tag{7}$$

The frictional force can be converted to the pressure on the membrane by dividing by the surface area of the cell. The surface area is treated as being constant during osmotic efflux (the lateral compressibility of lipid bilayers is limited (Evans and Skalak, 1980), thus this assumption is reasonable).

$$\mathscr{P} = \frac{\mathrm{kT}}{\mathrm{AD_w}} \cdot J_w \cdot \Delta x \tag{8}$$

$\mathscr{P}$ is pressure on the membrane due to water flux (N/m^2) and A is surface area of the cell (m^2).

Prediction of membrane rupture under water flux stress

Eq. 8 describes the pressure exerted on the plasma membrane as a result of water flux through the membrane. The question now is whether the magnitude of this pressure is sufficient to rupture biological membranes.

The behavior of the membrane is similar to a fluid or plastic material and cannot, therefore, be thought of as a rigid body that suddenly breaks when this pressure exceeds a critical value. If we consider a single cell with a uniform pressure being exerted on the membrane, a local membrane rupture may be viewed as a spontaneous symmetry breakdown, caused by local fluctuations in the tensile strength of the membrane. There will be an average breaking strength for the entire surface of the membrane, however, local variations will occur. The average rate at which a fluctuation of a given magnitude (reflecting a change in the breaking strength) occurs in a specific locality will be constant over long time periods, although the occurrence of individual events will be random and uncorrelated with the history of this location. Thus we can define a mean rate at which fluctuations (of a given strength) occur

$$\alpha = \lim_{t \to \infty} \left[\frac{n}{t} \right] \tag{9}$$

where n is the number of fluctuations which occur in time t, t is the time interval under consideration, and α is the average rate of occurrence of fluctuations of a given strength.

Let us now consider an incrementally longer time interval $(t + \Delta t)$ in which we make Δt very small so that on average, it is unlikely that a fluctuation will occur in Δt. In this case, the probability of finding a fluctuation in Δt is

$$P(1, \Delta t) \ll 1. \tag{10}$$

Probability is defined as the limit that is reached of the number of occurrences per repetition as the number of repetitions becomes infinitely large; thus the probability of finding at least one occurrence in this very small time interval is related to the average rate of spontaneous fluctuation occurrence by

$$P(1, \Delta t) = \alpha \cdot \Delta t. \tag{11}$$

Therefore, the probability that a fluctuation does not occur in Δt is

$$P(0, \Delta t) = [1 - P(1, \Delta t)]. \tag{12}$$

The probability that no fluctuations occur in time t is found by breaking t into $t/\Delta t$ intervals of length Δt. The probability that no fluctuations occur in t is then the product of the probabilities that no fluctuations occur in each of the intervals of length Δt

$$P(0, t) = [P(0, \Delta t)]^{t/\Delta t}. \tag{13}$$

Since,

$$P(0, \Delta t) = (1 - \alpha \cdot \Delta t), \tag{14}$$

then,

$$P(0, t) = \lim_{\Delta t \to 0} \left[1 - \alpha \cdot t \left(\frac{\Delta t}{t} \right) \right]^{t/\Delta t}. \tag{15}$$

By definition, the natural exponential function can be expressed as

$$e^{-x} = \lim_{N \to \infty} \left[1 - \frac{x}{N} \right]^N. \tag{16}$$

Therefore, corresponding $t/\Delta t$ to N, we are left with

$$P(0, t) = e^{-\alpha \cdot t}. \tag{17}$$

The probability that a fluctuation occurs in time t is therefore

$$P(1, t) = 1 - e^{-\alpha \cdot t}. \tag{18}$$

The rate at which fluctuations occur with a given strength is given by a constant

$$\alpha = \text{constant}. \tag{19}$$

Since α is a rate constant, it can be replaced with the more widely used time constant, τ

$$\alpha = 1/\tau. \tag{20}$$

Thus the probability that a fluctuation of a given strength occurs is given by

$$P(1, t) = 1 - e^{-t/\tau}. \tag{21}$$

There is also a probability of finding a fluctuation of a given

strength (the local breaking strength where the fluctuation occurs) at a particular location at one instant in time. The distribution of fluctuations of a given strength over the area of the membrane can be expected to form a normal distribution about some mean value. For a given force being placed on a local area of the membrane, the probability that this pressure will exceed the local breaking strength of the membrane will be given by the integral of the binomial distribution. This can be approximated to a high degree of accuracy by a two parameter logistic equation

$$P_{\mathscr{P}>\mathscr{P}_c} = \frac{1}{1 + e^{-b(\mathscr{P}-\bar{\mathscr{P}})}} \tag{22}$$

where $\mathscr{P}$ is the probability that the force placed on the membrane exceeds the local breaking strength, $\mathscr{P}$ is pressure imparted on the membrane, $\mathscr{P}_c$ is the pressure which will exceed the local breaking strength of the membrane, $\bar{\mathscr{P}}$ is the mean strength of the membrane (average pressure required for failure), and b is a parameter related to the standard deviation of the membrane strength distribution (b = 1.70991/σ, where σ = standard deviation).

The probability that a given force (which is constant with time) exceeds the breaking strength of the membrane as a function of time is therefore given by the product of the probability that the force exceeds the breaking strength of the membrane and the probability that a fluctuation of the required strength has occurred

$$P_{\text{rupture}} = \left[\frac{1}{1 + e^{-b(\mathscr{P}-\bar{\mathscr{P}})}}\right][1 - e^{-t/\tau}] \tag{23}$$

The three parameters in Eq. 23 will have a temperature dependence as they describe a mechanical failure of the lipid bilayer which is stabilized by hydrophobic interactions and Van der Waal's forces (the strengths of which are functions of temperature). This temperature dependence should be adequately described by an Arrhenius relation

$$\bar{\mathscr{P}}\,(\mathrm{T}) = \mathscr{P}_g \cdot \exp\left[\frac{E_a}{R}\left(\frac{1}{T_g} - \frac{1}{T}\right)\right] \tag{24}$$

where $\mathscr{P}_g$ is the mean pressure required for failure at the reference temperature, E_a is Arrhenius activation energy, R is the universal gas constant, T is absolute temperature, and T_g is the reference temperature.

Experimental estimates of water flux were calculated from the rate of change in cell volume in response to a gradient in osmotic pressure across the plasma membrane. A cryomicroscope was used to experimentally monitor water flux and the incidence of IIF during freezing. The critical water flux resulting in intracellular freezing was used in Eq. 8 to calculate the pressure imparted on the membrane. This critical pressure was compared to results from other studies in which membrane failure was achieved by hydrostatic pressure gradients. If IIF is a result of a rupture of the plasma membrane, then it is reasonable to expect that the pressure due to water flux (at the magnitude of water flux that correlates with the formation of IIF) should be comparable to the hydrostatic pressure that is required to rupture plasma membranes in situations in which there are no osmotic pressure gradients.

MATERIALS AND METHODS

The Chinese Hamster fibroblast cells (V79-w, derived from lung tissue) used in this study were grown in tissue culture using minimal essential medium (GIBCO, Grand Island, NY) with Hanks' salts, 25 mM 4-(2-hydroxyethyl)-1-piperazineethanesulfonic acid buffer (GIBCO), 10% fetal calf serum (GIBCO), 0.4% sodium bicarbonate, 100 μg/ml penicillin/streptomycin, and 2 mM L-glutamine. The cells were maintained in exponential growth phase by harvesting from plastic tissue culture dishes (75 cm^2; Corning Glass Works, Corning, NY) with regular trypsinization (0.25% trypsin (GIBCO) for 10 min at 37°C) and resuspension in tissue culture medium.

Microscopic observations of cells at subzero temperatures were made using a computer-controlled convection cryomicroscope stage described previously (Muldrew and McGann, 1990). A 2-μl sample of cell suspension was placed under a cover slip on the cryomicroscope stage, and all observations were made within 0.5 mm of the thermocouple junction to minimize the effects of thermal gradients. The stage was cooled to a specified subfreezing temperature and held at that temperature, while ice formation was initiated at the edge of the cover slip. Measurements showed that the latent heat of fusion resulted in a maximum temperature increase of 0.5°C, which was buffered in less than 1.5 s, which was small compared to the time required for shrinkage. The stage was held at the constant temperature for 1 min following ice formation. Experiments were recorded on videotape for later analysis. The presence of intracellular ice was assayed by observing the sudden darkening of the cytoplasm. Measurements of volume change with time were made by digitizing the images from videotape (TARGA+ digitizing board; Truevision, Inc., Indianapolis, IN) and then using a custom computer program to determine the cross-sectional area of the cell and calculating an equivalent spherical cell volume.

RESULTS

Fig. 1 shows the dependence of IIF on the temperature of ice nucleation. Intracellular ice begins to appear when the temperature of nucleation is below −4°C. The proportion of cells freezing intracellularly increases rapidly as the nucleation temperature is lowered, with all the cells undergoing IIF at

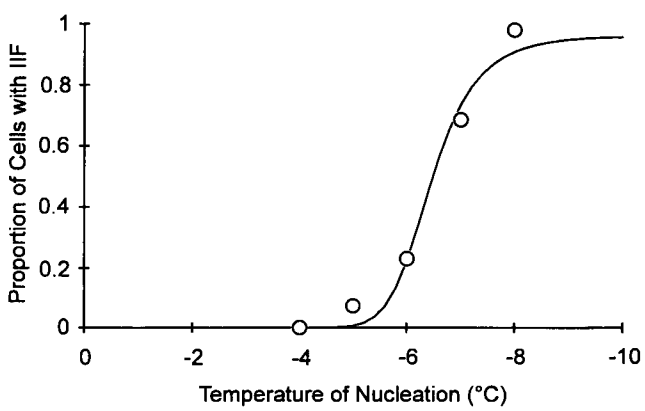

FIGURE 1 Intracellular ice formation in hamster fibroblasts. The proportion of cells which "flashed" on ice nucleation at predetermined temperatures. Between 50 and 64 cells were observed for each experimental point. The solid line is a least squares fit of Eq. 23 with $\bar{\mathscr{P}}$ = 75.6 N/m^2 (activation energy = 18.5 kcal/mol), b = 0.3 (activation energy = −18.5 kcal/mol), and τ = 0.5 s (activation energy = −18.5 kcal/mol) at −4°C.

nucleation temperatures below −8°C. The kinetics of cell volume change are shown in Fig. 2 for nucleation temperatures of −2 and −4°C. There is a wide range of permeabilities within a homogeneous population of cells, so measurement of shrinkage at nucleation temperatures where IIF occurs could be biased by removing the cells which undergo IIF from the population of shrinking cells (i.e., if the cells which lose water slowly are more likely to undergo IIF, then removing these from the sample would bias the average towards a higher permeability). The experimental data in Fig. 2 were fit to equations describing water loss (described in more detail elsewhere (McGann et al, 1988)) which were adapted from the work of Dick (1966). The equations describe the water flux driven by the osmotic pressure gradient which develops during freezing.

$$\frac{dV}{dt} = L_p \cdot A \cdot R \cdot T \cdot (\pi_i - \pi_e) \qquad (25)$$

where dV/dt is the rate of volume change, L_p is hydraulic conductivity, A is the cell surface area, R is the gas constant, T is the temperature, π_e is osmotic pressure of the suspending medium (calculated from the phase diagram of sodium chloride and water (Cocks and Brower, 1974)), and π_i is osmotic pressure of the cytoplasm, where the osmotic pressure of the cytoplasm during shrinkage can be expressed in terms of the cell volume using the Boyle–van't Hoff relation applied to the osmotic responses of cells (Lucke and McCutcheon, 1932).

$$\pi_i = \pi_o \frac{1 - v_d}{v - v_d} \qquad (26)$$

where π_o is the isotonic osmotic pressure, v is the normalized cell volume, and v_d is the osmotically inactive fraction of cell volume.

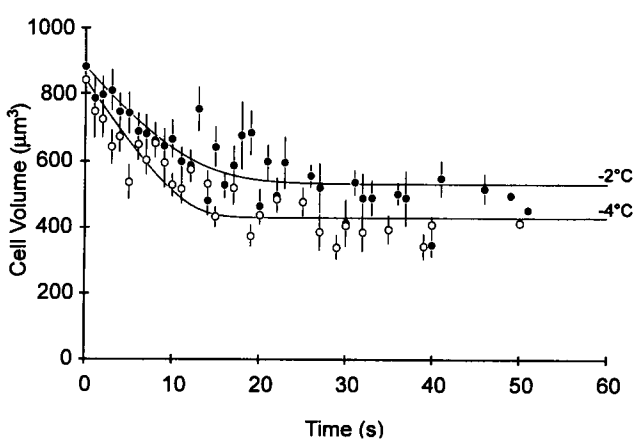

FIGURE 2 Osmotic shrinkage of hamster fibroblasts after nucleation of ice at −2 and −4°C. The closed circles show the average values of cell volume after nucleation of ice at −2°C, and the open circles represent the average volume following ice nucleation at −4°C. The solid lines show the least squares fit of an equation for osmotic water flux (see text). The fit was accomplished using the simplex method. The initial slope of the line for −2°C is 29 $\mu m^3/s$ and for −4°C is 38 $\mu m^3/s$.

For hamster fibroblasts, values of the hydraulic conductivity and osmotically inactive fraction, derived by fitting experimental data to Eqs. 25 and 26, are shown in Table 1. Also shown in this table are values of the permeability parameters for liposomes and oocytes, taken from the literature, which are to be used in the discussion. The values of L_p and v_d thus obtained enable us to use Eqs. 25 and 26 to simulate the kinetics of water loss due to osmotic pressure gradients. The experimental data points and the curves generated using the best-fit values for the parameters are shown in Fig. 2. The magnitude of water flux is maximal immediately upon ice formation as this is when the osmotic pressure gradient is greatest; therefore, the peak rate of water flux can be obtained by taking the initial slope of the curve generated from the fitted parameters. The peak water flux at −2°C was 30 $\mu m^3/s$, increasing to 38 $\mu m^3/s$ at −4°C when IIF begins to occur (as shown in Fig. 1). The hydraulic conductivity of the plasma membrane (and hence the water flux) decreases with decreasing temperature so there is a temperature at which the increase in osmotic stress (due to a decrease in the nucleation temperature) is balanced by the decrease in hydraulic conductivity. At lower temperatures, the water flux will decrease with decreasing nucleation temperature; thus it is important to show that the magnitude of the peak water flux is increasing at temperatures at which IIF begins to occur.

DISCUSSION

Experimental measurements of water flux

Since the rate of water efflux is still increasing at −4°C, the water flux that occurs in the range over which damage occurs (see Fig. 1) will be greater than the 38 $\mu m^3/s$ that was measured. This value is simply being used to show that the water flux which is associated with IIF generates a frictional drag on the membrane that is within the range of forces that has been shown to cause rupture from hydrostatic pressures. Although the difference between the upper and lower boundaries that were chosen for this study represent a wide range of values, it is important to establish the feasibility of the hypothesis by this method. The precision of estimates of the critical pressure will be significantly enhanced in the discussion when the hypothesis will be used to analyze a published account of the IIF behavior of liposomes. The critical pressure which causes rupture (and hence IIF) in liposomes can be compared directly to the hydrostatic pressure needed to rupture pure lipid bilayers.

Forces required to rupture membranes

Studies of planar lipid bilayers have found that a difference in hydrostatic pressure of 1×10^{-4} atm leads to a rupture of a bilayer spanning a 1-mm diameter circular opening (Jain, 1972). Micropipette suction experiments on red blood cells have found that pressure differences of 0.1 atm are sufficient to rupture the membrane when it is being suctioned into a 3-μm diameter micropipette (Evans and Skalak, 1980). We

TABLE 1 Permeability parameters

	V_{iso}*	V_d	L_p	E_a	T_g	Ref.
	μm^3	$\times V_{iso}$	$\mu m^3/\mu m^2 \cdot min \cdot atm$	kcal/mol	K	
Fibroblasts	885	0.44	0.241		271	
Fibroblasts	845	0.42	0.118		269	
Oocytes	2.30×10^5	0.018	0.43	13–14.5	295	Leibo (1980)
Oocytes	2.62×10^5	0.214	0.044	13.3	273	Toner, Cravalho, Armant (1990)
Liposomes	4189	0.06	1.82	10.6	295	Callow and McGrath (1985)

* V_{iso}, isotonic volume.

can take these values as the approximate lower and upper limits of hydrostatic pressures needed to rupture a plasma membrane of mammalian cells (a simple lipid bilayer will likely represent the lower limit since there are no structures to add stability; the red cell membrane, with its extensive cytoskeleton, is a reasonable choice for the upper end of the spectrum). These values were used in Eq. 8 to determine the critical water flux (the water flux which imparts a pressure on the plasma membrane (due to friction) which is sufficient to rupture the membrane). This critical flux will be compared with the experimentally measured water flux at the beginning of the range over which damage occurs (38 $\mu m^3/s$ at −4°C in hamster fibroblasts).

The surface area of the hamster fibroblast cells is assumed to remain constant during swelling and shrinkage and is taken as the surface area of a sphere (isotonic volume = 865 μm^3; therefore surface area = 417 μm^2). The diffusion coefficient for water in liquid hexadecane has been measured at several temperatures (Schatzberg, 1965), giving an Arrhenius activation energy of 3.35 kcal/mol, allowing calculation of the diffusion coefficient at −4°C (2.26×10^{-9} m^2/s). The width of the hydrophobic region of the bilayer (Δx) is commonly taken as 50 Å (Fettiplace et al., 1971), so the critical water flux for hamster fibroblasts can then be calculated using these values in Eq. 8. The lower limit is 5.6×10^{11} molecules/s (or 17.1 $\mu m^3/s$) and the upper limit is 5.6×10^{14} molecules/s (or 1.71×10^4 $\mu m^3/s$).

The experimentally measured water flux (at the onset of IIF) is 38 $\mu m^3/s$, which is just above the bottom end of the calculated range. The magnitude of the peak water flux will continue to increase as the temperature of ice nucleation is lowered due to the increased osmotic pressure gradients that will be generated. Fig. 1 shows that the proportion of cells undergoing IIF also increases. This concordance establishes the feasibility of the osmotic rupture hypothesis; however, without detailed measurements of the hydrostatic pressure required to rupture hamster fibroblast membranes, this data cannot be taken any further. To further investigate the implications of the hypothesis, and to subject it to more rigorous testing, we have undertaken to apply it to other systems in which IIF has been studied. By generalizing the approach so that quantities that have been measured for various cell types can be used to predict the onset of IIF, a comparison can be made between predictions of the theory and experimental results.

Application of the theory

The theory can be used to predict membrane rupture due to osmotic water flux if the conditions under which rupture occurs are known. For the case in which membrane rupture occurs during rapid cooling (indicated by IIF), Eq. 23 can be readily applied to any cell type for which the permeability parameters and the conditions under which IIF occurs are known. The shrinkage data for the fibroblasts shown in Fig. 2 provided estimates of the hydraulic conductivity and the osmotically inactive volume which can be used with the water flux equations to predict the peak water flux which occurs on nucleation at subfreezing temperatures (the temperature range over which shrinkage measurements were carried out (2°C) is not large enough to determine a reasonable estimate of the Arrhenius activation energy for the hydraulic conductivity, so the value was assumed to be the same as that measured for mouse oocytes, 13.3 kcal/mol, cited by Leibo (1980) and Toner et al. (1990)). Fig. 1 shows the measured proportion of cells which undergo IIF on nucleation at several temperatures which can be used with Eq. 23 to generate estimates of the membrane rupture parameters. This is done by a least squares fit in which the errors to be squared and summed are the differences between the P_{IIF} from Eq. 23 and the measured proportion of cells undergoing IIF at each temperature for which a measurement exists. Fig. 1 shows the results of this fit as a solid line. The estimates of the membrane rupture parameters can then be used to predict rupture under any circumstance in which the osmotic stresses can be defined.

To demonstrate the utility of this approach, two cases from the literature will be discussed. The first system that will be analyzed is that of unilamellar liposomes, as described by Callow and McGrath (1985). The behavior of liposomes during freezing is similar to that of cellular systems and they present a simple model system in which the critical pressure is known (this value was presented as the lower boundary for rupture earlier (10^{-4} atm), which was taken from data describing pure lipid bilayers (Jain, 1972)). Thus the critical water flux can be inserted into Eq. 8 to compare the pressure due to friction which is associated with IIF and the hydrostatic pressure that causes rupture of a lipid bilayer.

IIF in liposomes

The relevant permeability parameters for the liposomes are summarized in Table 1. The activation energy is from Blok

et al. (1977) as it is midway between the other two values cited in Callow and McGrath (1985). The osmolality of the hypertonic sucrose solution during freezing is taken from the CRC Handbook of Chemistry and Physics (Weast, 1985). The surface area of the liposomes is treated as the surface of a shrinking sphere in the simulations of freezing behavior as this is the assumption that was used to fit the parameters to the original data (Callow and McGrath, 1985). The equations used to model osmotic water efflux are the same as those used for the fibroblasts discussed earlier. Fig. 3 shows the water flux as a function of temperature for each of the four cooling rates which define the conditions of IIF for liposomes (Callow and McGrath, 1985). Using the values of water flux given in Fig. 3, the parameters of Eq. 23 ($\bar{\mathscr{P}}$, b, and τ) were fit to minimize the sum of squared errors between the measured and predicted proportion of cells undergoing IIF using an assumed activation energy for these parameters of 5 kcal/mol (−5 kcal/mol for b and τ as they are expected to decrease with temperature; this has the effect of making the membrane more fragile at lower temperatures). Table 2 shows the measured and predicted percentages of cells with IIF as a function of cooling rate. The measured values are taken from Callow and McGrath (1985).

The predicted probability of IIF from Eq. 23 is shown in Fig. 4 (the predicted values in Table 2 are the final values in this figure) which can also be used to predict the temperature at which IIF occurs. The mean temperature at which IIF should occur is between −3 and −5°C which is close to the measured value of −5°C (Callow and McGrath, 1985). The magnitude of water flux at −4°C which correlates to 5% IIF (57 $\mu m^3/s$) can be directly inserted into Eq. 8 (after converting to molecules/s) to get the pressure due to friction that is associated with this flux. ($k = 1.38 \times 10^{-23}$ Nm/K, $T = 269$ K, $A = 1257\ \mu m^2 = 1.257 \times 10^{-9}\ m^2$, $D_w = 2.26 \times 10^{-9}\ m^2/s$, $J_w = 57\ \mu m^3/s = 1.9 \times 10^{12}$ molecules/s

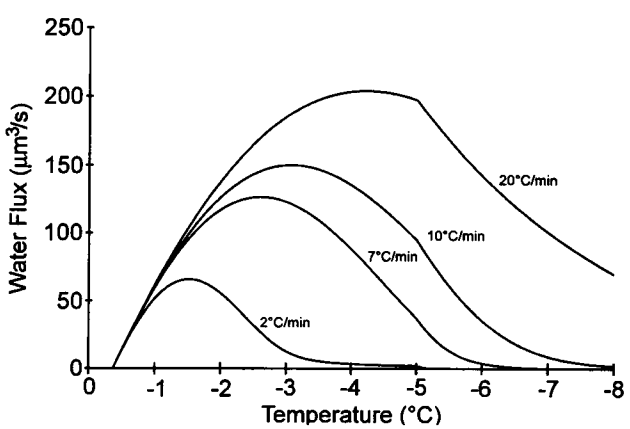

FIGURE 3 Rate of water efflux from liposomes during constant cooling. The instantaneous rate of water efflux is plotted as a function of temperature for the four different cooling rates (2, 7, 10, and 20°C/min) for liposomes in a 0.2 M sucrose solution. The water flux is calculated from the water transport equation in response to the increased osmolality of the unfrozen solution due to ice formation. The discontinuity occurs at the eutectic temperature of a water-sucrose solution.

TABLE 2 Intracellular ice formation in liposomes

Cooling rate	Measured IIF	Predicted IIF
°C/min	%	%
2	0	1
7	34	33
10	70	71
20	100	97

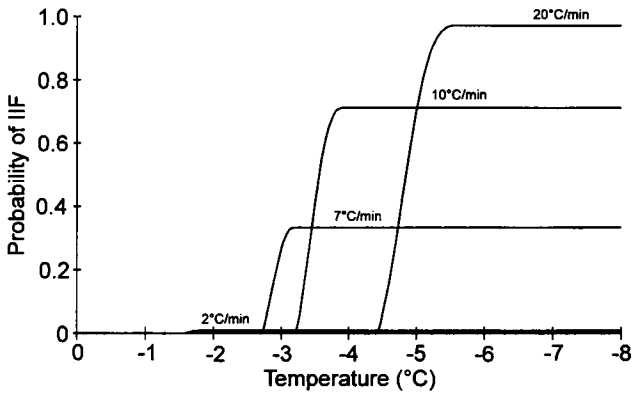

FIGURE 4 Probability of IIF in liposomes during constant cooling. The probability of IIF in liposomes is shown as a function of temperature reached during cooling at four different cooling rates (2, 7, 10, and 20°C/min). The maximum values reached are summarized in Table 2. The parameters used to determine these curves are: $\bar{\mathscr{P}} = 27.5\ N/m^2$ (activation energy = 5 kcal/mol), $b = 0.30$ (activation energy = −5 kcal/mol), and $\tau = 10$ s (activation energy = −5 kcal/mol).

(1 molecule of water = $3 \times 10^{-11}\ \mu m^3$), and $\Delta x = 5 \times 10^{-9}$ m.) Thus, the critical pressure, $\mathscr{P} = 12.4\ N/m^2$ (1.23×10^{-4} atm).

The critical pressure which causes damage at the 5% level is 1.23×10^{-4} atm, just above the value of 1×10^{-4} atm of hydrostatic pressure which causes planar lipid bilayers to rupture (Jain, 1972). Table 2 shows that Eq. 23 is able to describe IIF in liposomes phenomenologically. The strength of the theory, however, is clearly seen when the water flux which is associated with IIF (predicted by fitting to experimental data) is inserted into Eq. 8 to calculate the pressure that is put on the membrane from this water flux. The pressure due to the frictional drag of water moving osmotically (at the level of water flux that is associated with rupture) is the same as the hydrostatic pressure that causes rupture.

IIF in mouse oocytes

Leibo et al. (1978) first quantified IIF in mouse oocytes and later, Leibo (1980) measured the permeability parameters for these cells. Toner, et al. (1990) have recently published detailed cryomicroscopic studies of IIF in mouse oocytes along with permeability data for these cells (Toner et al., 1990) which is in agreement with that of Leibo. The relevant permeability parameters are listed in Table 1. Using the phase diagram for sodium chloride and water (Cocks and Brower, 1974) to predict the extracellular concentration of solutes as a function of temperature, the water flux during freezing was

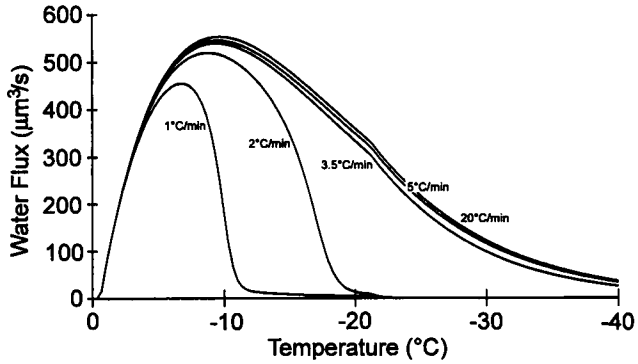

FIGURE 5 Water efflux from mouse oocytes during constant cooling. Water flux from mouse oocytes is shown as a function of temperature for five different cooling rates (1, 2, 3.5, 5, and 20°C/min). The permeability parameters used to calculate these fluxes are from Toner et al. (1990) and are listed in Table 1. The discontinuity occurs at the eutectic temperature of a water-sodium chloride solution.

simulated for the cooling rates which produce IIF (the equations for modeling water movement are the same as in the previous example). Fig. 5 shows the water flux as a function of temperature for these five cooling rates (predicted from the parameters in Table 1 applied to the equation for water movement). The parameters for membrane rupture ($\overline{\mathscr{P}}$, b, and τ) were fitted to these predicted values, minimizing the sum of squared errors between the measured (Toner et al., 1990) and predicted incidence of IIF (the predicted incidence of IIF is from Eq. 23). The values of these parameters that gave the best fit, as well as the percentage of cells undergoing IIF, are presented in Table 3.

Fig. 6 shows the predicted probability of IIF for these cooling rates and can be used to predict the mean temperature at which IIF occurs (between −11 and −13°C) which compares favorably to the measured values between −12 and −15°C (Toner et al., 1990). Rall et al. (1983) performed cryomicroscope experiments on mouse embryos and found that the temperature at which IIF occurred was significantly depressed in the presence of cryoprotectants. This phenomenon can be accounted for precisely with the osmotic rupture hypothesis (the cryoprotective additives reduce the magnitude of water flux at a given temperature), but, because of the difficulties in describing multicellular structures and modeling osmotic responses in the presence of permeating cryoprotectants, the treatment will not be performed in this paper.

TABLE 3 Intracellular ice formation in mouse oocytes

Cooling Rate	Measured IIF	Predicted IIF ($\overline{\mathscr{P}}$ = 9.0 N/m²; b = 0.90; τ = 30.0 s)
°C/min	%	%
1	0	21
2	65	81
3.5	88	95
5	100	97
20	100	100

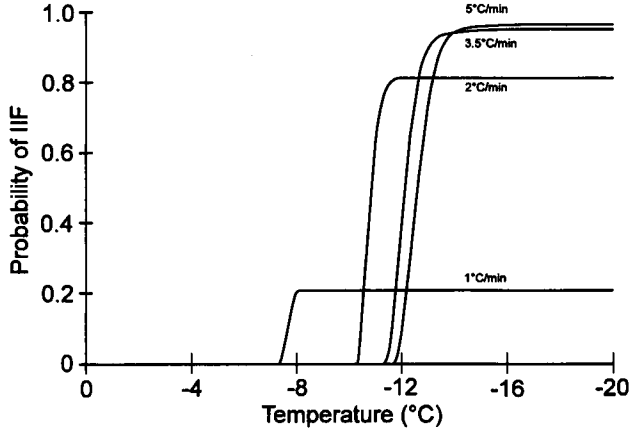

FIGURE 6 Probability of IIF in mouse oocytes during constant cooling. The cumulative probability of IIF in mouse oocytes is plotted as a function of temperature for four cooling rates (1, 2, 3.5, and 5°C/min). The maximum values reached are summarized in Table 3. The parameters used to determine these curves are: $\overline{\mathscr{P}}$ = 9.0 N/m² (activation energy = 5 kcal/mol), b = 0.90 (activation energy = −5 kcal/mol), and τ = 30 s (activation energy = −5 kcal/mol).

The values of the critical water flux parameters derived from this data can also be used to predict the incidence of IIF for isothermal experiments (these are experiments in which the cells are either cooled extremely rapidly to a specified subzero temperature or supercooled to this temperature and then subjected to freezing followed by a holding period during which the incidence of IIF is observed). Fig. 7 shows this prediction as well as several points taken from the measured data (Toner et al., 1990). The fit is very good, showing once again that the theory provides an excellent description of the phenomenology of intracellular ice formation.

Other phenomena associated with IIF

There is an effect associated with IIF in which cells that were rapidly frozen can remain viable if the warming rate is also

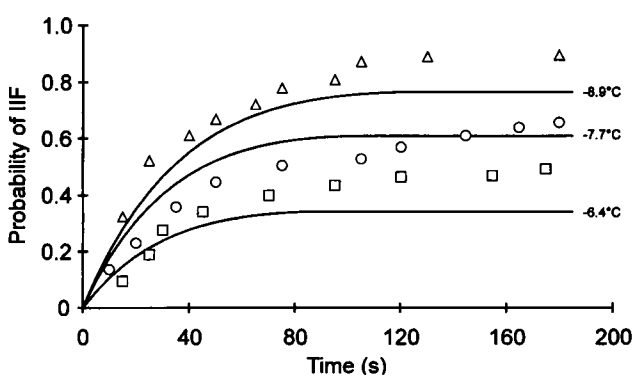

FIGURE 7 Probability of IIF in mouse oocytes during isothermal freezing. The probability of IIF for mouse oocytes during isothermal experiments (the cells are cooled very rapidly to a specified temperature and then held at that temperature for several minutes) are plotted as a function of time. The solid lines represent the predicted probability of IIF (using the parameters that were fit to data from the cooling rate experiments modeled in Figs. 6 and 7). The shapes are several points taken from the actual data (Toner et al., 1990) which are representative of the measured response.

rapid (Mazur, 1960; Mazur et al., 1972; McGann and Farrant, 1976). This effect is usually ascribed to the lack of time for recrystallization of intracellular ice (recrystallization is the process by which large ice crystals with low surface energy grow at the expense of small ice crystals with high surface energy). In the present theory, IIF results in an ice structure which extends through a hole in the membrane (where the rupture occurred). Therefore, recrystallization could cause this transmembrane extension to enlarge in radius thereby further damaging the membrane (the possibility of small holes resealing is the mechanism by which rapidly warmed cells might survive). An alternate view (Rall et al., 1894) attributes warming rate sensitivity of rapidly cooled cells to the vitrification of the cytoplasm during cooling, and subsequent devitrification at low rates of warming. During warming of rapidly cooled cells, at low temperatures above the glass transition temperature, the gradient in osmotic pressure driving water from the cell remains. Therefore conditions for membrane damage due to water flux persists during warming until the melting of ice reduces, then reverses the movement of water across the membrane.

A further implication of this theory is that a cell which has been cooled slowly to some subfreezing temperature could be challenged with high, potentially damaging, gradients in osmotic pressure during rewarming. In practice, rapid warming (which would lead to the highest osmotic pressure gradients) is usually beneficial (Mazur, 1977), presumably due to the fact that maximum water flux occurs after ice has melted, at higher temperatures where the membrane is less fragile.

A trend can be seen in the literature in which cells with high values of L_p are able to tolerate faster cooling rates without undergoing IIF (Mazur, 1984). From this hypothesis, it must be supposed that a necessary precondition of having a high water permeability, is the possession of a membrane architecture that is able to withstand the stress associated with osmotic water movement. The presence of aqueous pores in the membrane is an example of such a modification of membrane architecture. The correlation between high values of L_p and the ability to withstand large water fluxes and hence rapid cooling is, therefore, due to the evolutionary necessity of cells being able to withstand osmotic stresses which would otherwise be lethal. The red blood cell provides an excellent model for comparison to test this idea, however, since the primary route for water movement is through pores (Finkelstein, 1987), this treatment will have to await a further extension of the theory.

Cell injury can be induced by osmotic stresses in the absence of ice which appear to be of the same form as the injury associated with IIF (Muldrew and McGann, 1990). The osmotic stresses required to elicit this injury appear also to be of the magnitude that would be predicted from the osmotic rupture hypothesis (Muldrew and McGann, 1990). In fact, the activation energy for the water flux that causes 50% of the cells to rupture has been measured for hamster fibroblasts and has a value of 22.1 kcal/mol (McGann and Muldrew, 1992). The temperature dependence of plastic flow in red blood cell membranes has an activation energy of 18.6 kcal/mol (Waugh, 1982). If we use this value for the activation energy of the critical frictional force in Eq. 7 (plastic flow is due to a force, not a pressure, so Eq. 7 is used), the resulting activation energy of the critical water flux is 21 kcal/mol (due to the facts that diffusion of water within the membrane has an activation energy of 3.35 kcal/mol and temperature is also a parameter in the equation). There is currently no other hypothesis of the causes of IIF that can explain this injury; furthermore, with the recent trend to using extremely high concentrations of cryoprotectants to create vitrification solutions, the necessity of predicting osmotic injury at temperatures above freezing has taken on an increased importance. The addition and removal of these cryoprotective compounds is problematic for cell suspensions and very difficult for tissue systems. With the ability to model injury (using the present hypothesis) as a result of osmotic stresses created during addition of high levels of cryoprotectants, it may be possible to optimize protocols without spending excessive time conducting trial and error experiments.

CONCLUSION

The osmotic rupture hypothesis of cryoinjury was introduced to explain the phenomenon of intracellular freezing due to the failure of prevailing theories to account for several experimental challenges (Muldrew and McGann, 1990). The principal criticism of the hypothesis, following its introduction, was that the cause of injury was ascribed to osmotic pressure gradients across the plasma membrane. Osmotic pressure is simply a property of a solution; it is not a hydrostatic pressure and critics could not see how it could lead to a rupture in a plasma membrane. This was acknowledged in the initial paper and it was suggested that the water flux that was driven by the osmotic pressure gradient could be the factor by which a physical force was imparted to the membrane during dehydration. In the present report, this idea was formalized and shown to be not only plausible, but, taken with the evidence presented in the initial paper (Muldrew and McGann, 1990), quite likely.

The importance of discovering the mechanisms by which cellular injury occurs during cryopreservation cannot be overstated. With the continuing failure to cryopreserve large mammalian tissues and organs, researchers need a new paradigm. One of the most promising is the use of mathematical models in which cryopreservation protocols can be tested without having to perform lengthy and difficult experiments. Until recently, however, there have not been any theories of cryoinjury in which the onset of damage could be correlated with specific physico-chemical events which occur during freezing and thawing (see Toner et al. (1990) for an alternative hypothesis of IIF which is conducive to modeling). The osmotic rupture hypothesis links injury to osmotically driven water flux which is a parameter that can be modeled accurately. There have already been several complex models developed to predict the osmotic responses within tissue and organ systems (Bischof and Rubinsky, 1991; Diller et al.,

1991), however, these have been restricted by the lack of theories of cryoinjury that could be used within these models. It is hoped that this new hypothesis will be used in such a manner to allow new approaches to cryopreservation to be discovered.

REFERENCES

Bacic, G., R. Srejic and S. Ratkovic. 1990. Water transport through membranes: a review of NMR studies of model and biological systems. *Stud. Biophys.* 138:95–104.

Bischof, J., and B. Rubinsky. 1991. Mathematical models for the process of freezing in tissue. *Cryobiology.* 28:558.

Blok, M., L. VanDeenen, and J. DeGier. 1977. The effect of cholesterol incorporation on the temperature dependence of water permeation through liposomal membranes prepared from phosphatidylcholines. *Biochim. Biophys. Acta.* 464:509–518.

Callow, R., and J. McGrath. 1985. Thermodynamic modeling and cryomicroscopy of cell-size, unilamellar, and paucilamellar liposomes. *Cryobiology.* 22:251–267.

Chalmers, B. 1959. How water freezes. *Sci. Am.* 200:114–122.

Cocks, F., and W. Brower. 1974. Phase diagram relationships in cryobiology. *Cryobiology.* 11:340–358.

Denker, B., B. Smith, F. Kuhajda, and P. Agre. 1988. Identification, purification and partial characterization of a novel M_r 28,000 integral membrane protein from erythrocytes and renal tubules. *J. Biol. Chem.* 263: 15634–15642.

Dick, D. 1966. Cell Water. Butterworth, Inc., Wash. DC. pp. 83–89.

Diller, K., F. Merchant, and C. Lauchenbruch. 1991. Network thermodynamic simulation of combined osmotic and mechanical behavior of pancreas islets during cryopreservation. *Cryobiology.* 28:587–588.

Dowgert, M., and P. Steponkus. 1983. Effect of cold acclimation on intracellular ice formation in isolated protoplasts. *Plant Physiol.* 72: 978–988.

Einstein, A. 1956. Investigations on the theory of the Brownian Movement. R. Furth, editor. Dover Publications, Inc.

Evans, E., and R. Skalak. 1980. Mechanics and Thermodynamics of Biomembranes. CRC Press, Inc., Boca Raton, FL. p. 146.

Fettiplace, R., D. Andrews, and D. Haydon. 1971. The thickness, composition and structure of some lipid bilayers and natural membranes. *J. Membr. Biol.* 5:277–296.

Finkelstein, A. 1987. Water Movement Through Lipid Bilayers, Pores, and Plasma Membranes. John Wiley & Sons, Inc., New York. 12–13, 93–106, 155–183.

Jain, M. 1972. The Bimolecular Lipid Membrane: A System. Van Nostrand Reinhold, New York, p. 54.

Leibo, S. 1980. Water permeability and its activation energy of fertilized and unfertilized mouse ova. *J. Membr. Biol.* 53:179–188.

Leibo, S., J. McGrath, and E. Cravalho. 1978. Microscopic observation of intracellular ice formation in mouse ova as a function of cooling rate. *Cryobiology.* 15:257–271.

Levitt, D. 1974. A new theory of transport for cell membranes pores I. General theory and application to red cell. *Biochim. Biophys. Acta.* 373: 115–131.

Lucke, B., and M. McCutcheon. 1932. The living cell as an osmotic system and its permeability to water. *Physiol. Rev.* 12:68–132.

Mazur, P. 1960. Physical factors implicated in the death of micro-organisms at subzero temperatures. *Ann. NY Acad. Sci.* 85:610–629.

Mazur, P. 1963. Kinetics of water loss from cells at subzero temperatures and the likelihood of intracellular freezing. *J. Gen. Physiol.* 47:347–369.

Mazur, P. 1966. Physical and chemical basis of injury in single-celled microorganisms subjected to freezing and thawing. In Cryobiology. H. T. Meryman, editor. Academic Press, New York. pp. 213–315.

Mazur, P. 1977. The role of intracellular freezing in the death of cells cooled at supraoptimal rates. *Cryobiology.* 14:251–272.

Mazur, P. 1984. Freezing of living cells: mechanisms and implications. *Am. J. Physiol.* 247:C125–C142.

Mazur, P., W. Rall, and S. Leibo. 1984. Kinetics of water loss and the likelihood of intracellular freezing in mouse ova: influence of the method of calculating the temperature dependence of water permeability. *Cell Biophys.* 6:197–214.

Mazur, P., S. Leibo, and E. Chu. 1972. A two factor hypothesis of freezing injury. *Exp. Cell Res.* 71:345–355.

McGann, L., and J. Farrant. 1976. Survival of tissue culture cells frozen by a two-step procedure to −196°C. II. Warming rate and concentration of dimethyl sulfoxide. *Cryobiology.* 13:269–273.

McGann, L., M. Stevenson, K. Muldrew, and N. Schachar. 1988. Kinetics of osmotic water movement in chondrocytes isolated from articular cartilage and applications to cryopreservation. *J. Orthop. Res.* 6:109–115.

McGann, L., and K. Muldrew. 1992. Temperature dependence of membrane sensitivity to osmotic stresses. *Cryobiology.* 29:786–787.

Muldrew, K., and L. E. McGann. 1990. Mechanisms of intracellular ice formation. *Biophys. J.* 57:525–532.

Pitt, R., and P. Steponkus. 1989. Quantitative analysis of the probability of intracellular ice formation during freezing of isolated protoplasts. *Cryobiology.* 26:44–63.

Preston, G., T. Carroll, W. Gugginno, and P. Agre. 1992. Appearance of water channels in *Xenopus* oocytes expressing red cell CHIP28 protein. *Science (Wash. DC).* 256:385–387.

Rall, W. F., D. S. Reid, and C. Polge. 1894. Analysis of slow-warming injury of mouse embryos by cryomicroscopical, and physiological methods. *Cryobiology.* 21:106–121.

Rall, W., P. Mazur, and J. McGrath. 1983. Depression of the ice-nucleation temperature of rapidly cooled mouse embryos by glycerol and dimethyl sulfoxide. *Biophys. J.* 41:1–12.

Rubinsky, B., and D. Pegg, 1988. A mathematical model for the freezing process in biological tissue. *Proc. R. Soc. Lond.* B234:343–358.

Schatzberg, P. 1965. Diffusion of water through hydrocarbon liquids. *J. Polymer Sci.* (No. 10, Pt. C):87–92.

Steponkus, P., and M. Dowgert. 1981. Gas bubble formation during intracellular ice formation. *Cryo-Lett.* 2:42–47.

Steponkus, P., and M. Dowgert. 1981. Phenomenology of intracellular ice nucleation in isolated protoplasts. *Plant Physiol.* 67(suppl.):58

Toner, M., M. Karel, and E. Cravalho. 1990. Thermodynamics and kinetics of intracellular ice formation during freezing of biological cells. *J. Appl. Phys.* 67:1582–1593.

Toner, M., E. Cravalho, and D. Armant. 1990. Water transport and estimated transmembrane potential during freezing of mouse oocytes. *J. Membrane Biol.* 115:261–272.

Toner, M., E. Cravalho, and M. Karel. 1990. Cellular response of mouse oocytes to freezing stress: prediction of intracellular ice formation. *J. Biomech. Eng.* 115:169–174.

Waugh, R. E. 1982. Temperature dependence of the yield shear resultant and the plastic viscosity coefficient of erythrocyte membrane. *Biophys. J.* 39:273–278.

Weast, R. (editor-in-chief) 1985. CRC Handbook of Chemistry and Physics, 66th edition. CRC Press, Inc., Boca Raton, FL. D262.

Zhang, R., K. Logee, and A. Verkman. 1990. Expression of mRNA coding for kidney and red cell water channels in *Xenopus* oocytes. *J. Biol. Chem.* 265:15375–15378.